Experimental study on deposition effect of Fe-based grouting inducers in silts

Zhaoyang Xu[a], Tingchun Bai, Jianzhang Huang, Yishan Pang and Feng Zhou

College of Civil Science and Engineering, Yangzhou University, Yangzhou, Jiangsu 225127, China

Abstract. This paper presents the Fe-based biological grouting in silt foundation to improve its engineering characteristics. The growing and enzyme activity of iron bacteria are measured. The effects of temperature and pH on the amount of Fe-based products are studied. The components of Fe-based deposits are investigated. Small-scale grouting testes are carried out and the distribution and variation of spatial pores in non-grouted and grouted silts are studied by CT scans. The filling effect of grouting is evaluated by small-scale shaking table tests on silt slope. The results show that Fe-based precipitations mainly consist of schwertmannite and had a small amount of crystal mineral $Fe_5(PO_4)_4(OH)_3 \cdot 2H_2O$. The deposits can fill the pores, leading to a reduction of porosity from 27.3% (non-grouting) to 10.2% (five-time grouting). The Fe-based deposit can effectively restrain the amplification effect of soil on the seismic waves. The proposed biological grouting method has application potential for the reinforcement of silt foundation.

Keywords: Fe-based grouting; deposition filling; CT scan; small-scale shaking table.

1 Introduction

As the mutual penetration and improvement of microbiology and basic and engineering science since the beginning of 21th century, biotechnologies have been gradually involved in the field of civil engineering. There are wide application prospects and significant engineering economic worth for the application of biotechnology in geotechnical engineering [1,2]. This technique can be used in foundation treatment such as the reinforcement of liquefied sand, reinforcement of weak subgrade, tunnel oriented reinforcement and slope protection of foundation pit[3].

The MICP (Microbially Induced Carbonate Precipitation) technique has been widely used in the soil reinforcement through biological grouting[4]. This is to form $CaCO_3$ induced from carbonate-mineralization microbes in the nutrient environment which is rich in calcium ions and nitrogen sources [5]. However, previous studies show that the microbes have strong vitalities only in the alkaline environment with a pH of 8.0~9.0 and the process is complex in practice [6].

In the natural environment, iron bacteria can obtain the energy necessary for its reproduction by autotrophic or heterotrophic effects which in turn produce precipitation of iron compound. Chu et al. oxidized the Fe^{2+} to Fe^{3+} by iron bacteria taken from sludge. The obtained ferric hydroxide precipitation was then used to cement sands to strengthen the bond[7]. The reference[8] presented the application of iron oxide strain for the grouting of silty soil. The permeability of the grouted silt was

[a] Corresponding author : zhaoyang_xu@aliyun.com

reduced by two levels which enhanced its unconfined compressive strength, dynamic strength and dynamic shear strength. Iron bacteria can be applied not only for reinforcement and modification of soil but dealing with environmental heavy metal pollution, meeting the requirements of sustainable development [9].

This paper applied a type of iron bacteria separated from soil to biologically grout silts using the metabolism products. The deposition and filling effects of Fe-based grouting in silts were studied by micro analyses and small-scale shaking table tests.

2 Biological experiments

2.1 Growing and enzyme activity of iron bacteria S1968

The tested iron bacteria were obtained from common silty clay. The test results of 16SrDNA of iron bacteria were compared to the available data in GenBank. It was found that the bacteria had a 98.9% similarity to the Arthrobacter niigatensis. The bacteria were sent to China microbial culture collection center, labelled as S1968.

The media of iron bacteria S1968 had 10g of ammonium ferric citrate, 0.5g of magnesium sulfate, 0.5g of ammonium ferrous sulfate, 0.5g of dipotassium hydrogen orthophosphate, 0.5g of sodium nitrate, 0.2g of calcium chloride, pH of 6.8~7.0 per liter. The precipitation of Fe-based compound was produced by the self-metabolism of iron bacteria, as shown in Figure 1.

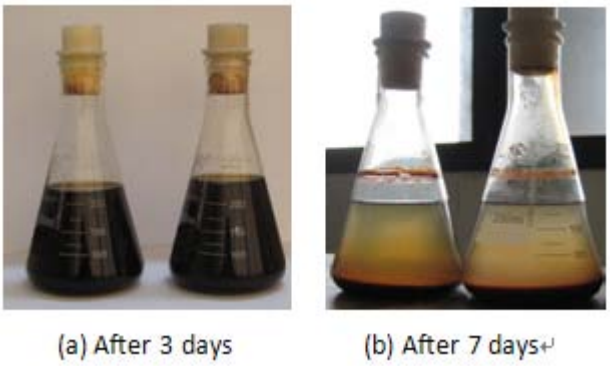

Figure 1. Formation process of sediment

The amount of microorganism was measured by 752-type visible range spectrophotometer with a wave length of 700nm. The measurements were expressed as OD_{700}. The variation of conductivity of bacterial liquid was monitored by conductivity meters. The enzyme produced in the self-metabolism may decompose and transform the previous electrically conductive organic nutrients to non-conductive Fe-based compound which reduced the conductivity of the liquid. Therefore, the conductivity of bacteria liquid reflected the activity of enzyme of iron bacteria.

Based on the 1% inoculation rate, the mother liquid of iron bacteria was inoculated to 50ml nutrient fluid and cultured in a shaking table under a constant temperature for 96h. The OD_{700} and average conductivity of bacteria liquid were measured timely.

Figure 2 shows the conductivity-time curve. It can be seen that there was a sharp reduction of conductivity between 24h and 48h, indicating a rapid growing of the enzyme activity. During 48h~54h, the variation of conductivity became gradually steady where the decomposition of nutrients by bacteria basically ended. There appeared a small amount of flocculation in red brown (i.e. Fe-based compound) in the liquid. There was no variation in the conductivity after 54h which represented the end of metabolism.

Figure 3 shows the variation of iron bacteria S1968. The comparison between Figures 3 and 4 shows that the sharp increment of measured ODs were due to the increasing turbidity and reducing

conductivity of bacteria liquid resulting from the decomposition of nutrients by bacteria and production of Fe-based compound. The compound started to aggregate and deposit after a certain concentration level, leading to an obvious layering of bacteria liquid. The metabolism of bacteria ended after 54h and thus the OD became steady.

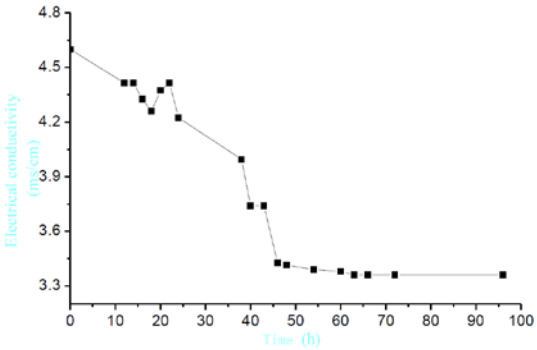

Figure 2. Variation of conductivity of bacteria liquid against time.

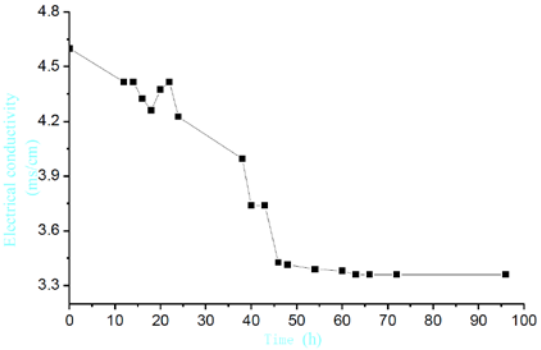

Figure 3. Variation of OD_{700} of bacteria liquid against time.

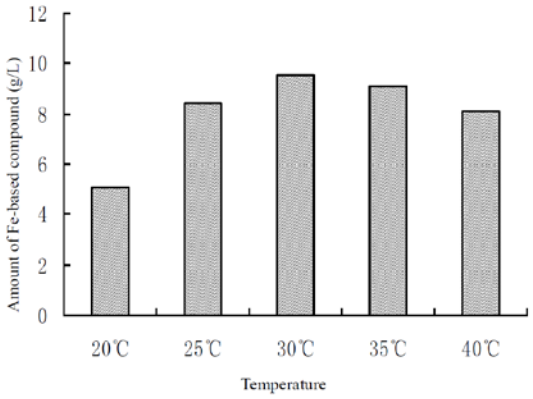

Figure 4. Variation of Fe-based sediments against Temperature.

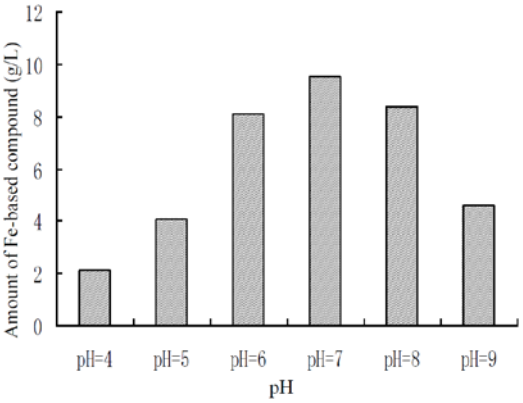

Figure 5 . Variation of Fe-based sediments against pH

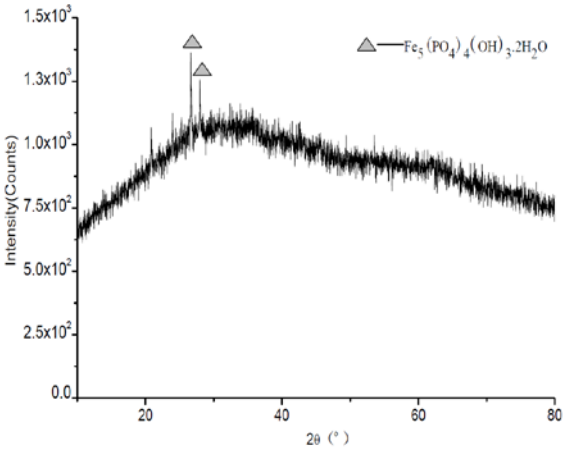

Figure 6 . XRD pattern of bio-metabolites

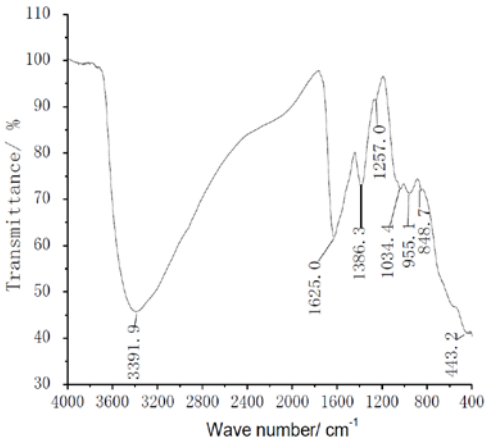

Figure 7 . FTIR spectrum of bio-metabolites

1.2 Impact of temperature and pH on Fe-based Sediments

Figures 5 and 6 show the amount of produced Fe-based sediments in 300ml liquid with 4% inoculation for different temperatures and pHs, respectively. The initial pH of bacterial liquid was 7.0 and the temperature was kept constant as 30°C. The sediment reached its maximum value at 30°C. For pH of 4.0~5.0, there was a small amount of sediments, indicating that it was not suitable for bacteria to grow under acidic conditions. There was a larger amount of sediments for pH of 6.0~8.0 with a maximum value for pH=7.0.

1.3 XRD and FTIR analyses of Fe-based compound

The XRD and FITR tests were carried out after the filtration and drying of Fe-based sediments to study the crystal form and composition of mineral. The XRD spectrum in Figure 6 shows a relatively bad crystal form of sediments which mainly composed of amorphous material. There was also some crystal mineral $Fe_5(PO_4)_4(OH)_3 \cdot 2H_2O$. The FTIR in Figure 7 shows that the peak location and feature of infrared ray spectra of Fe-based compound agreed well with that of schwertmannite. Compared to the standard sample of schwertmannite listed in Table 1, it was found that all the absorption peaks of Fe-based complex can belong to schwertmannite.

Table 1. IR absorbance characteristics of standard and synthetic schwertmannite

Substance	OH stretch	H_2O deformation	SO_4	FeO_6
Standard schwertmannite	3318	1629	702-1118	432
Fe-based complexes	3391.9	1625.0	848-1034	443.2

2 Experiment and analysis of small-scale bio grouting in silt

2.1 Test layout of grouting

The basic characteristics of the tested silts were listed in Tables 2 and 3. Figure 8 shows the layout of grouting. The grouting was conducted in a syringe with an inner diameter of 40mm. The volume of silts was 100ml (height of 80mm). Before grouting, 30ml deionized water was input to saturate the silt. The silt sample was set for 24h at room temperature of 26±2°C. before grouting.

The process of Fe-based grouting: injected 30ml bacteria liquid cultured for 52h into the silt sample at a speed of 5~10mL/min and discharged filtrate after 1h's setting, repeated this process for another two times for a total injection of 90ml. The liquid was set for 24h and repeated this grouting process for five times. The sample was labelled as A-2, compared to the non-grouted silt sample A-1.

Table 2. Main performance parameters of silts

Specific gravity of silt particle Gs	Plastic limit ω_P	Liquid limit ω_L	Plastic limit index Ip	Maximum dry density g/cm^3	Best moisture content w_{op}%
2.70	20.5%	28.9%	8.4	1.52	25.6

Table 3. Composition of silts

Grain composition (mm)	2~0.5	0.5~0.25	0.25~0.075	0.075~0.005	<0.005
silt	0%	0.2%	16.6%	76.3%	6.9%

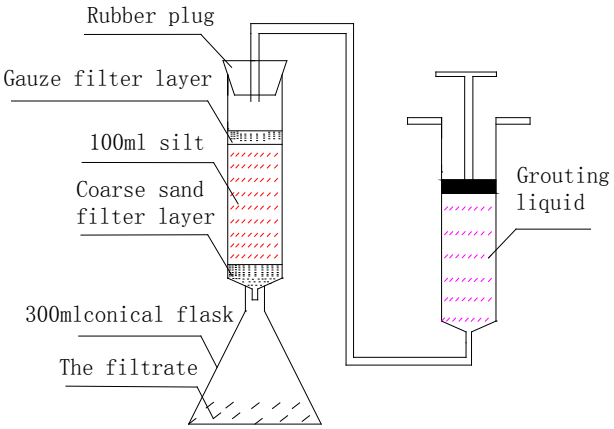

Figure 8 . Model of grouting

2.2 CT scan analysis of grouted silts

CT scans were conducted on A-1 and A-2 to better reflect the filling effect of Fe-based grouting.

Figures 9 and 10 show the CT scan results of A-1 and A-2, respectively. The figure (a) shows the 3D pore distribution with a size sequence of red-orange-yellow-green-blue (from large size to small size). It can be seen that the sample A-1 had more pores most of which were connected and the silt particles were in a loose state. After the grouting, there were reduced large pores which accorded to the observations in the vertical section (figure b) and transverse section (figure c).

The porosity is the most important index to reflect the filling effect. The porosity of 5-time grouting silts (A-2) was 10.2%, a reduction by 62.6% compared to a porosity of 27.3% of A-1. This indicates the possibility of Fe-based biological precipitation in silts and good filling effect.

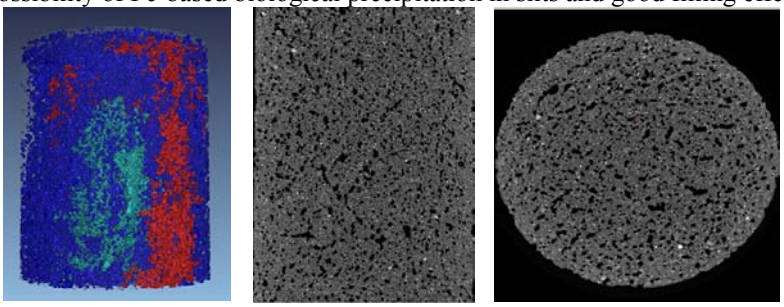

(a) 3D pore distribution (b) profile (c) cross-section

Figure 9. CT scan images of A-1

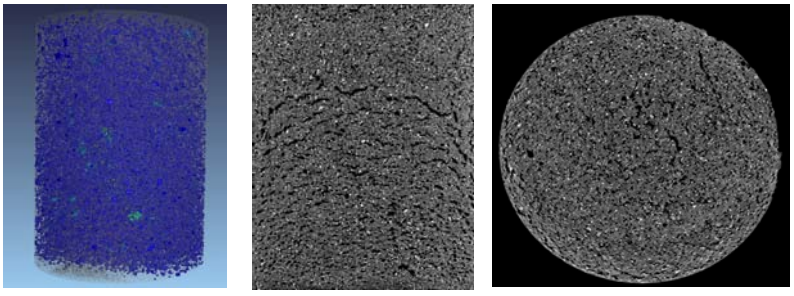

(a) 3D pore distribution (b) profile (c) cross-section

Figure 10. CT scan images of A-2

3 Slope shaking table test on grouted silts

3.1 Biological grouting of silt slope

Small-scale shaking table tests were carried out to investigate the filling effect of Fe-based grouting by observing the failure modes and acceleration of non-grouted and grouted silts. The tested mold was 40cm×22cm×40cm (length × width × height). The same silts as Section 2.1 were used. The silt slope was built by excavation from a full fill soil, and had a height of 22cm and a slope-to-height ratio of 1:1.36.

The biological grouting was conducted on the silt foundation through drilling holes by PVC tube under a pressure of 10~50kPa, as shown in Figure 11. After the grouting, the foundation soil was cut to form a soil slope where the shaking table tests were conducted. The 10Hz sinusoidal wave was input as the vibration excitation for 30s.

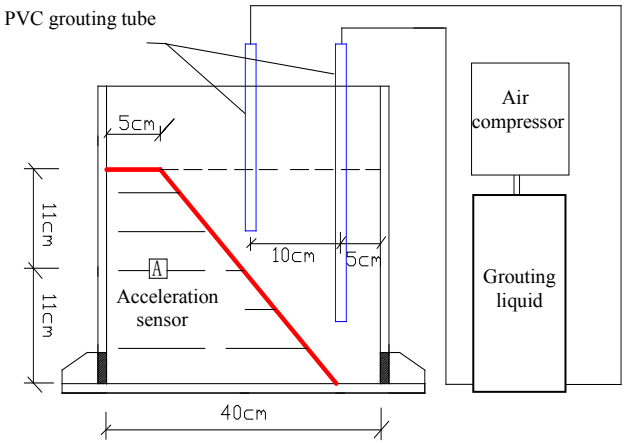

Figure 11. Schematic of grouting

3.2 Results of shaking table tests

Figures 12 and 13 show the failure modes of non-grouted and Fe-based grouted silt slopes under seismic loading, respectively. For non-grouted silt slope, there appeared many cracks in the interior at 7~8s. The cracks extended as the seismic shear stress transferred. Collapse occurred in a large range at about 25s. The peak settlement reached 7cm at 30s. In contrast, there was no global collapse for grouted silt slope. The failure developed from the peak to the foot of slopes and parallel to the slope. There was a 2cm peak settlement at 30s.

Figure 12. Failure of silt slope without grouting

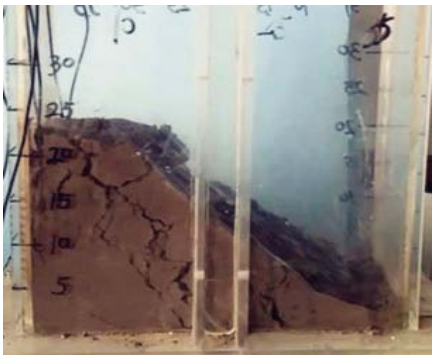

Figure 13. Failure of silt slope with grouting

Figure 14 shows the acceleration history of seismic waves with an average value of 0.2g. Figures 15 and 16 show the field acceleration histories of non-grouted and Fe-based grouted silt slopes, respectively. For non-grouted silts, the amplification factor of acceleration peak (the ratio of peak of silt acceleration to the input peak seismic acceleration) was 7.09. This value was significantly reduced to 3.86 for grouted silts. This indicates that the filling of Fe-based deposit after grouting can restrain the amplification effect of foundation on seismic waves.

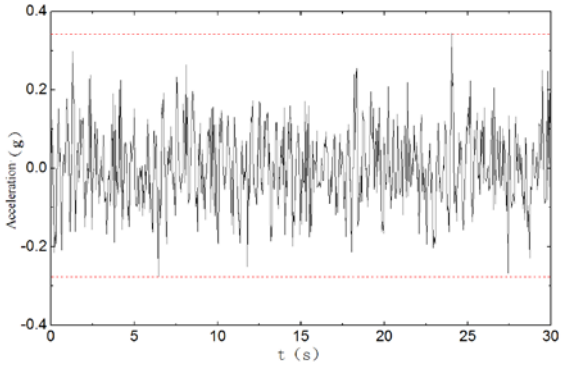

Figure 14. Variation of acceleration of seismic waves against time

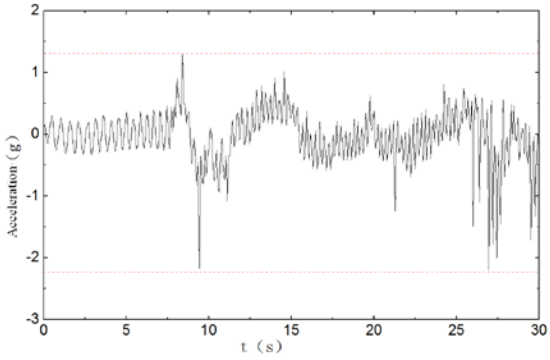

Figure 15 . Variation of acceleration of non-grouted silt against time.

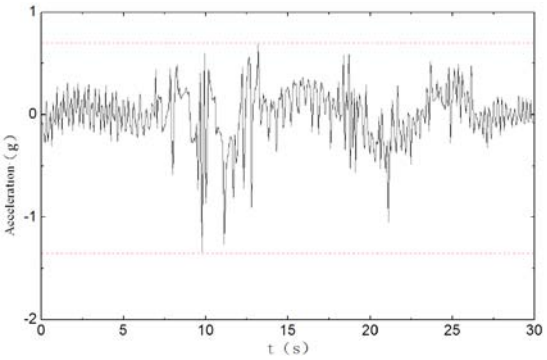

Figure 16 . Variation of acceleration of grouted silt against time.

4 Conclusions

(1) For inoculation ratio of 1% and 50ml nutrient liquid, the 12h~48h was a logarithmic growth period of iron bacteria S1968. The enzyme activity experienced a rapid increment during 24h~48h. The deposit started to appear at 48h and ended after 54h.

(2) There were more deposits induced from iron bacteria S1968 in the environment of temperature of 25°C~40°C and pH of 6.0~8.0. The maximum deposit can be obtained at 30°C and pH=7.0.

(3) The crystal form of sediment was not obvious with a small amount of crystal mineral $Fe_5(PO_4)_4(OH)_3 \cdot 2H_2O$. The FTIR analysis showed good agreement of the peak location and feature of infrared ray spectra between the Fe-based compound and schwertmannite.

(4) The Fe-based grouting in silts can produce the bio-induced deposition in the small-scale micro porous silts and effective filling of pores. Under the same vibration loading, the Fe-based deposits can effectively restrain the amplification effect of soil on seismic waves, and thus contribute to the decay of seismic waves and enhance the dynamic characteristics of foundations.

Acknowledgements

This work was supported by National Natural Science Foundation of China (Project No.51278446) and Jiangsu Natural Science Funds (Project No.BY2016069-05).

References

1. L.A.Van Paassen, V.S.Whiffin, M.P.Harkes, GEOMICROBIOL.J, **24**, 417-423 (2007).
2. M.P.Harkes, L.A.Van Paassen, J.L.Booster, V.S.Whiffin, M.C.M.Van Loosdrecht, ECOL ENG, **36**,112-117(2010).
3. L.A.Van Paassen, Geo-Frontiers Congress, **2**, 4099-4108(2011).
4. J.De Jong, B.Mortensen, B.Martinez, et al, ECOL ENG, **36**, 197-210(2010).
5. L.A.Warren, P.A.Maurice, N.Parmar, F.G.Ferris, GEOMICROBIOL.J, **18**, 93-115(2001).
6. M.Li, X.H.Cheng, H.X.Guo. INT BIODETER BIODEGR, **76**, 81-85(2013).
7. J.Chu, V.Ivanov, J.He, et al, Geo-Frontiers Congress, **211**, 4070-4078(2011).
8. Z.Y. Xu, F.Zhou, T.C.Bai, et al, J.PURE APPL MICROBIO, **9**, 1899-1905(2015).
9. Z.Y. Xu, Y.R.Ma, F.Zhou, et al, J.PURE APPL MICROBIO, **7**, 336-339(2013).

